Received: 26 December 2019 | Revised: 10 April 2020 | Accepted: 12 May 2020

DOI: 10.4218/etrij.2019-0595

ORIGINAL ARTICLE

ETRI Journal WILEY

Distributed beamforming with one-bit feedback and clustering for multi-node wireless energy transfer

Jonghyeok Lee[1] | **SeongJun Hwang**[1] | **Yong-gi Hong**[1] | **Jaehyun Park**[1] | **Woo-Jin Byun**[2]

[1]Department of Smart Robot Convergence and Application Engineering, Pukyong National University, Busan, Rep. of Korea

[2]Radio Satellite Research Division, Electronics and Telecommunications Research Institute, Daejeon, Rep. of Korea

Correspondence
Jaehyun Park, Pukyong National University, Busan, Rep. of Korea.
Email: jaehyun@pknu.ac.kr

Funding information
This work was supported in part by the Electronics and Telecommunications Research Institute, which is funded by the Korean government under Grant 20ZH1100, "Study on 3D Communication Technology for Hyper-connectivity." It was also supported in part by the Basic Science Research Program through the National Research Foundation of Korea, which is funded by the Ministry of Education (2018R1D1A1B07043786).

Abstract

To resolve energy depletion issues in massive Internet of Things sensor networks, we developed a set of distributed energy beamforming methods with one-bit feedback and clustering for multi-node wireless energy transfer, where multiple single-antenna distributed energy transmitters (Txs) transfer their energy to multiple nodes wirelessly. Unlike previous works focusing on distributed information beamforming using a single energy receiver (Rx) node, we developed a distributed energy beamforming method for multiple Rx nodes. Additionally, we propose two clustering methods in which each Tx node chooses a suitable Rx node. Furthermore, we propose a fast distributed beamforming method based on Tx sub-clustering. Through computer simulations, we demonstrate that the proposed distributed beamforming method makes it possible to transfer wireless energy to massive numbers of sensors effectively and rapidly with small implementation complexity. We also analyze the energy harvesting outage probability of the proposed beamforming method, which provides insights into the design of wireless energy transfer networks with distributed beamforming.

KEYWORDS

distributed beamforming, wireless energy transfer, wireless powered sensor network

1 | INTRODUCTION

Recently, wireless sensor networks have become a major focus in various machine-to-machine or Internet of Things (IoT) applications, such as home networking, military, and healthcare applications. Because sensor nodes are typically battery powered, energy-efficient data transmission schemes and routing protocols have been studied extensively ([1–3] and the references therein). Additionally, there has been significant interest in transferring energy wirelessly. To overcome the energy depletion of sensor nodes, wireless energy transfer networks have been deployed in combination with conventional wireless communication networks [4–7]. However, because the efficiency of wireless energy transfer decreases significantly over large transmission distances, multiple-antenna–based energy transmission techniques have been investigated extensively [8–11]. In [8], a radio frequency (RF) energy beamforming method with multiple antennas was developed. In [9], RF energy transmission using multiple antennas was demonstrated experimentally. However, these works assumed that multiple transmitting antennas can be collocated and processed coherently for RF energy beamforming. This assumption is not

applicable to scenarios in which energy transmitters (Txs) are distributed in IoT sensor networks. In [10,11], with consideration for wireless powered IoT senor networks, scheduling strategies for RF energy transmission were investigated to minimize the required transmitted energy to prevent energy depletion in IoT sensor networks. However, although distributed RF Txs were considered in [10–12], cooperation among distributed Txs was not considered. In [13] and [14], energy resource allocation strategies for IoT sensor networks were developed based on heuristic algorithms and the bat algorithm. Although these studies did not consider wireless RF energy transfer in IoT sensor networks, the developed resource allocation and scheduling methods can be extended and integrated into our proposed energy transfer strategies to resolve the energy depletion problem in IoT sensor networks.

In this paper, for wireless energy transfer networks in which there are multiple Txs and multiple senor nodes capable of harvesting energy wirelessly (energy receiver [Rx] nodes), we propose a distributed energy beamforming method with one-bit feedback and clustering. Distributed transmit beamforming is a well-known cooperative technique in wireless communications [15,16], where a plurality of "virtual" antennas are used to increase system capacity and transmission distance. Similarly, in the proposed paper, to transmit energy effectively, distributed energy Txs adjust their energy signal phases such that their signals are constructively added at Rx nodes with the same phase, resulting in increased received signal strength (RSS). It should be noted that in distributed beamforming with one-bit feedback, Txs do not require explicit channel state information (CSI), which reduces overall implementation complexity. For the sake of implementation simplicity, we consider that Txs transmit their RF energy signals only by adjusting their phases (see Figure 1). In contrast to previous works that focused on distributed information beamforming with a single Rx node [15,16], we developed a distributed energy beamforming method for multiple Rx nodes. Additionally, we propose two clustering methods in which each Tx chooses its serving Rx node. Because the harvested energy at an Rx node is inversely proportional to the path loss, we can develop a clustering method based on path loss, where each Tx can choose the serving node with the smallest path loss. However, because Txs cannot cooperate with each other in our distributed energy beamforming system, when using path-loss–based clustering, some Rx nodes may be selected by insufficient Txs, resulting in energy shortages. Accordingly, we propose another distributed clustering method, in which the number of actively serving Txs is reflected in the Rx node selection. Then, Tx nodes in the same cluster, which serve the same Rx node, can synchronize their phases in a distributed manner. As the number of Txs increases (ie, massively distributed Txs), through distributed beamforming with one-bit feedback [15], their phases are slowly synchronized, resulting in a long convergence time. Therefore, we also propose a fast distributed beamforming method based on Tx hierarchical sub-clustering. In this method, we separate the Txs within a cluster into several sub-clusters. In the first stage, the phases in each sub-cluster are synchronized via one-bit feedback. In the second stage, inter-sub-cluster phases are synchronized based on a grid search with one-bit feedback. By reducing the number of nodes to be synchronized within a sub-cluster, we can accelerate the distributed beamforming process for each sub-cluster, after which the inter-sub-cluster phases can be synchronized. We also analyze the energy harvesting outage probabilities of the proposed distributed beamforming method with clustering methods at Rx nodes, as well as the convergence time of the fast distributed beamforming with sub-clustering method. Through simulations, we verify that the proposed sub-clustering method reduces convergence time without any feedback overhead. Additionally, based on the results of energy outage probability analysis, we present insights into the design of wireless energy transfer networks with distributed beamforming. Considering a wireless powered IoT sensor network with distributed RF transmitters, the main contributions of this paper can be summarized as follows:

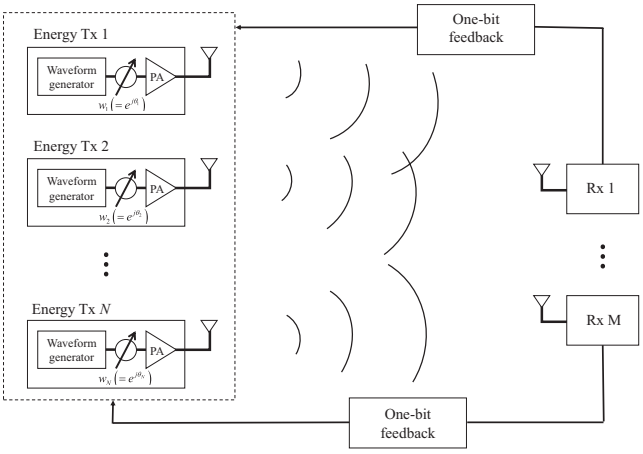

FIGURE 1 Distributed beamforming system with one -bit feedback

- Distributed beamforming with one-bit feedback is first proposed for RF energy transfer using multiple Rx nodes, where Txs do not require explicit channel state information, which reduces overall implementation complexity.
- For multiple nodes, we developed a path-loss–based clustering method in which each Tx can select an Rx node without requiring explicit CSI. Therefore, distributed energy beamforming with one-bit feedback can be processed within clusters. Additionally, we propose another distributed clustering method in which the number of active serving Txs is reflected in the Rx node selection. Because distributed Txs cannot cooperate with each other, when using path-loss–based clustering, some Rx nodes may be selected by insufficient Txs, resulting in energy outages/depletion. By using the proposed clustering method, we can further reduce energy outage probabilities.

- We also propose a fast distributed beamforming method based on Tx hierarchical sub-clustering. As the number of Txs increases (ie, massively distributed Txs), in distributed beamforming with one-bit feedback, their phases are slowly synchronized, resulting in a long convergence time. By reducing the number of nodes to be synchronized within a sub-cluster, we can accelerate the distributed beamforming process for each sub-cluster, followed by the synchronization of inter-sub-cluster phases. By evaluating the convergence time of the proposed fast distributed beamforming with sub-clustering method, we verify that our sub-clustering method reduces convergence time without any feedback overhead.
- Finally, we analyze the energy harvesting outage probabilities of the proposed energy beamforming method with two clustering methods theoretically by approximating the distribution of RSS values as a gamma distribution. The outage analysis results reveal that increasing node density is a more efficient manner of deploying wireless energy transfer networks with distributed beamforming compared to increasing the transmitted power at each Tx node. Additionally, we can determine how much Tx power is required to satisfy a given outage probability constraint, which is important for the design of wireless energy transfer networks with distributed beamforming.

The remainder of this paper is organized as follows: In Section 2, the system model considered in this paper is introduced. In Section 3, distributed beamforming with one-bit feedback is discussed. This method is applicable to the case of a single Rx node. In Section 4, by considering multiple Rx nodes, we propose two different clustering algorithms. In Section 5, fast distributed beamforming with one-bit feedback and hierarchical clustering is proposed for multiple Rx nodes. In Section 6, we present simulation results. Section 7 discusses our conclusions.

2 | SYSTEM MODEL

Figure 1 presents a distributed wireless energy transfer network, where N single-antenna Txs cooperatively send energy to M single-antenna nodes. Assuming a Rayleigh flat fading channel, the received signal $y_m(t)$ at the m-th node can be calculated as follows:

$$y_m(t) = \sum_{n=1}^{N} d_{m,n}^{-\alpha} h_{m,n} x_n(t) + v_m(t), \tag{1}$$

where $h_{m,n}$ is the channel from the n-th Tx to the m-th Rx node, which has a zero-mean complex Gaussian random variable (RV) with unit variance. $v_m(t)$ is a complex white Gaussian noise process with a variance of σ_n^2. Here, $d_{m,n}$ is the distance between the n-th Tx and the m-th Rx node. The path loss exponent and channel are assumed to be block-stationary, implying that the channel realization remains fixed within a coherent time duration. The transmit signal from the n-th Tx is denoted as $x_n(t)$, which is defined as

$$x_n(t) = w_n s(t), \tag{2}$$

where $s(t)$ is the i-th energy waveform with a signal period T_s and $w_n (= e^{j\theta_n})$ is the i-th phase-shifting weight for distributed beamforming (specifically, phase synchronization at the Rx nodes). It should be noted that $h_{m,n}$ in (1) can be rewritten as $h_m = a_{m,n} e^{j\phi_{m,n}}$, where $a_{m,n} \in \mathbb{R}^+$ has a Rayleigh distribution and $\phi_{m,n}$ is uniformly distributed in [0, 2π]. Accordingly, by substituting (2) into (1), we get

$$y_m(t) = s(t) \left(\sum_{n=1}^{N} d_{m,n}^{-\alpha} a_{m,n} e^{j(\phi_{m,n} + \theta_n)} \right) + v_m(t). \tag{3}$$

To maximize the RSS at the m-th node, the following condition should be satisfied.

$$(\theta_1 + \phi_{m,1}) = \cdots = (\theta_N + \phi_{m,N}) = \text{const.}, \tag{4}$$

which implies that the signals transmitted from multiple Txs are constructively added at the m-th Rx node with the same phase.

3 | DISTRIBUTED BEAMFORMING WITH ONE-BIT FEEDBACK FOR A SINGLE NODE

Motivated by [15] and [16], we developed a distributed energy beamforming method with one-bit feedback for a single Rx node. This node broadcasts a common message with single-bit feedback, and depending on the feedback bit, each Tx updates its transmitted signal phase. Throughout this paper, we assume that based on single-bit feedback, the feedback channel is error-free. For a single Rx node (ie, $M = 1$), the Txs proceed with the phase synchronization process, as described in Algorithm 1. It should be noted that $y_1[iT_s]$ in Step 5 can be expressed as

$$y_1(iT_s) = s(iT_s) \left(\sum_{n=1}^{N} d_{1,n}^{-\alpha} a_{1,n} e^{j(\phi_{1,n} + \theta_n[i])} \right) + v_m(iT_s), \tag{5}$$

where i_{converge} in Step 3 of the algorithm is introduced to check the convergence of the phase and terminate the algorithm. Specifically, if each Tx receives the feedback bits of consecutive zeroes, i_{converge} increases to $I_{\text{threshold}}$ (which was set to 200 in our simulations, but can be determined empirically) and it is determined that the optimal point has been reached, meaning the algorithm can be terminated. Because the Rx node can obtain

channel information easily, the optimal RSS can be calculated at the Rx node, meaning termination can be determined at the Rx node based on its optimal RSS.

Algorithm 1. Distributed energy beamforming for a single Rx node:

1. Initialize $\theta_n[0] = 0$ and $\theta_{n,\,\max}[0] = \theta_n[0]$ at the n-th Tx.
2. Initialize $\mathrm{RSS}_{1,\,\max}[0] = 0$ at the Rx node.
3. Set $i = 1$ and $i_{\mathrm{converge}} = 0$.
4. The n-th Tx transmits a signal with a phase $\theta_n[i] = \theta_{n,\,\max}[i-1] + \delta_\theta$, where δ_θ is uniformly distributed in $\left[-\pi/20, \pi/20\right]$.
5. If $\mathrm{RSS}_1[i] \geq \mathrm{RSS}_{1,\,\max}[i-1]$, then the Rx node updates $i_{\mathrm{converge}} = 0$ and $\mathrm{RSS}_{1,\,\max}[i] \geq \mathrm{RSS}_1[i]$, and broadcasts a feedback bit of one to the Txs, where $\mathrm{RSS}_1[i] = \left|y_1[i]\right|$ with $y_1[i] = y_1(iT_s)$.
6. Otherwise, the Rx node updates $i_{\mathrm{converge}} = i_{\mathrm{converge}} + 1$ and broadcasts a feedback bit of zero to the Txs.
7. If the n-th Tx receives a feedback bit of one, it updates $\theta_{n,\,\max}[i] = \theta_n[i]$.
8. If $i_{\mathrm{converge}} > I_{\mathrm{threshold}}$ with a constant $I_{\mathrm{threshold}}$, then terminate the algorithm.
9. Set $i = i + 1$ and return to Step 4.

4 | DISTRIBUTED CLUSTERING METHODS FOR MULTIPLE RX NODES IN A DISTRIBUTED BEAMFORMING SYSTEM WITH ONE-BIT FEEDBACK

When there are multiple Rx nodes in a given area, each Tx can select an Rx node and adjust its phase such that the transferred energy is maximized at the Rx node. Accordingly, the harvested energy at each Rx node depends on how the Txs are clustered to serve the Rx nodes.

4.1 | Clustering method based on path loss

It is assumed that both Tx and Rx nodes have information regarding the large-scale fading $d_{m,\,n}^{-\alpha}$ because path loss changes slowly and it is easy to acquire such long-term CSI. Each Tx can select the Rx node with the smallest path loss to achieve high energy transfer efficiency. Let $\bar{I}^M$ be a collection of sets $\bar{I}_m^M$ defined as

$$\bar{I}^M = \left\{\bar{I}_1^M, \ \ldots, \ \bar{I}_M^M\right\}, \tag{6}$$

where the cluster index set $\bar{I}^M = \{n_1^{(m)}, \ \ldots, \ n_{\bar{N}_m}^{(m)}\}$ is the set of Tx indices serving the m-th Rx node and $\bar{N}_m$ is the number of Txs serving the m-th Rx node. Then, the n-th Tx can select an Rx to serve such that $n \in \bar{I}_{\bar{m}}^M$ with

$$\bar{m} = \arg\max_m d_{m,\,n}^{-\alpha}. \tag{7}$$

After each Tx chooses an Rx node to serve (node selection phase), distributed beamforming can be performed according to Algorithm 1 in Section 3. In this manner, the Tx nodes included in $\bar{I}_m^M$ determine their weights (specifically, the phase θ_n of w_n in (2)) according to one-bit feedback from the m-th Rx node.

4.2 | Weighted clustering method based on path loss and the number of active serving Txs

In distributed beamforming with one-bit feedback, Txs cannot cooperate with each other and Txs must select Rx nodes to serve in a distributed manner, as indicated in (7). However, because each Tx selects the closest Rx node (smallest path loss) to achieve efficient energy transfer, some Rx nodes may be selected by insufficient Tx nodes, resulting in energy outages. Accordingly, we propose a novel distributed clustering method in which the number of active serving Txs is reflected in the clustering criterion. Specifically, we let $\tilde{I}^M$ be a collection of sets $\tilde{I}_{\tilde{m}}^M$ defined as

$$\tilde{I}^M = \left\{\%\tilde{I}_1^M, \ \ldots, \ \%\tilde{I}_M^M\right\}, \tag{8}$$

where the n-th Tx can select an Rx to serve such that $n \in \tilde{I}_{\tilde{m}}^M$ with

$$\tilde{m} = \arg\max_m \frac{d_{m,\,n}^{-\alpha}}{1 + \bar{N}_m}. \tag{9}$$

It should be noted that the number of Txs serving the m-th Rx node can be easily acquired by each Tx from the broadcasting signal of the m-th Rx node. In (9), when the number of active serving Txs is large, the cost function decreases and the n-th Tx can select an Rx node with a small number of serving Txs while maintaining a small path loss. Again, after each Tx chooses an Rx node to serve, distributed beamforming can be performed according to Algorithm 1 in Section 3.

Figure 2 presents an illustrative example of distributed clustering when there are three Rx nodes and 20 Tx nodes. Here, the Rxs are located at $(x, y) = \{(5, 5), (5, 15), \text{and } (15, 15)\}$ m. The Tx nodes are randomly placed in the range of $[0, 14] \times [0, 14]$ m. It should be noted that Tx nodes tend to be placed closer to the Rx at (5, 5) than to that at (15, 15) geometrically. Accordingly, when the Tx nodes are clustered according to (7), the Rx at (5, 5) is served by more Txs than the other Rxs, as shown in Figure 2A. In Figure 2B, the Tx nodes are clustered according to (9). One can see that the clustering boundaries (dashed lines in Figure 2) are slightly adjusted such that the Tx nodes are allocated in a more balanced manner.

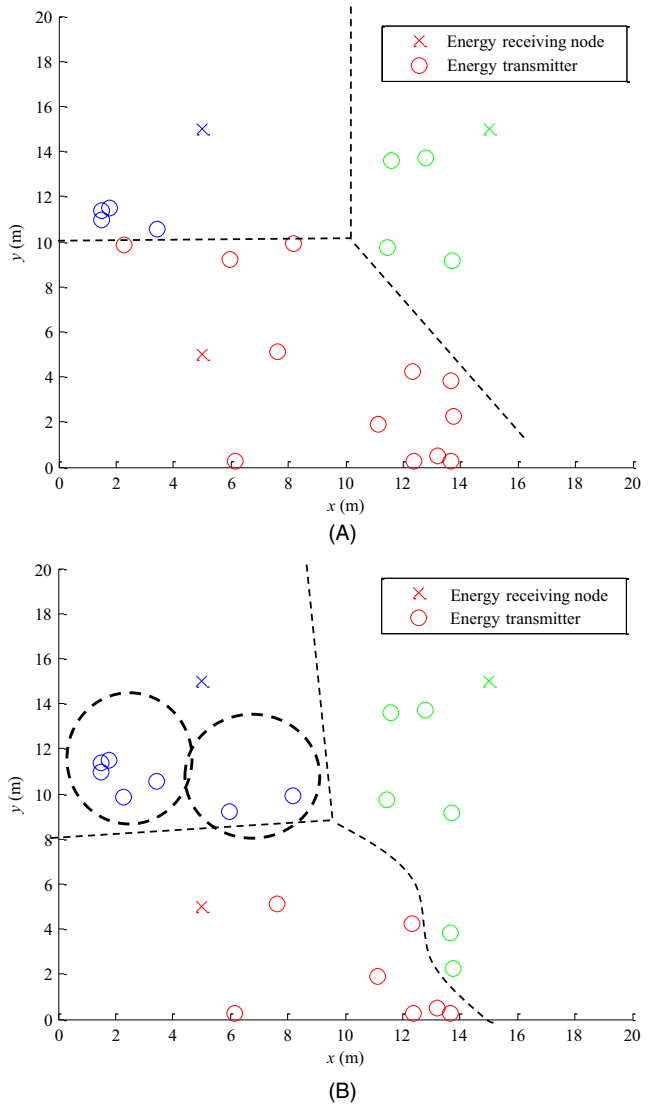

FIGURE 2 (A) Clustering based on (7) and (B) clustering based on (9)

5 | FAST DISTRIBUTED BEAMFORMING WITH ONE-BIT FEEDBACK AND HIERARCHICAL SUB-CLUSTERING FOR MULTIPLE RX NODES

In the previous section, we presented a clustering method to allow Txs to determine which Rxs they will serve (dashed lines in Figure 2). Because multiple Txs in the same cluster (ie, serving the same Rx node) adjust their phases according to one-bit feedback from the Rx node in a distributed manner, their phases slowly converge. Accordingly, we can create K sub-clusters of Tx nodes serving the same Rx node (dashed circle in Figure 2B). Then, in the first stage, the phases in each sub-cluster are synchronized according to one-bit feedback. In the second stage, inter-sub-cluster phases are synchronized based on a grid search with one-bit feedback.

Let $I^M = \{I_1^M, \ldots, I_M^M\}$ be a cluster set. Then, we create several sub-clusters from cooperative nodes in the same cluster. This process can also be performed without any central coordination. For example, to create K clusters, each node in the same cluster generates a random number p_m uniformly distributed in [0, 1]. If $p_m \in [(k-1)/K, k/K]$, then the m-th node belongs to the k-th sub-cluster. In Figure 2B, the cooperative nodes for the Rx at (5, 15) are separated into two sub-clusters ($K = 2$).

5.1 | Phase synchronization with one-bit feedback in each sub-cluster

After performing sub-clustering for the m-th cluster $\left(\tilde{I}_m^M = \{n_1^{(m)}, \ldots, n_{N_m}^{(m)}\}\right)$, the nodes in the k-th sub-cluster with $k = 1, \ldots, K$ proceed with the phase synchronization process, which is defined below.

Algorithm 2. Intra-sub-cluster phase synchronization for the m-th cluster:

1. Initialize $\theta_{n_k^{(m)}}[0] = 0$ and $\theta_{n_k^{(m)},\max}[0] = \theta_{n_k^{(m)}}[0]$ for each $n_k^{(m)}$, which is the Tx node index included in the k-th sub-cluster of the m-th cluster (serving the m-th Rx node).
2. Initialize $\mathrm{RSS}_{m,\,\max}[0] = 0$ at the data collector.
3. Set $i = 1$ and $i_{\text{converge}} = 0$.
4. The $n_k^{(m)}$-th Tx transmits a signal with a phase $\theta_{n_k^{(m)}}[i] = \theta_{n_k^{(m)},\max}[i-1] + \delta_\theta$, where δ_θ is uniformly distributed in $[-\pi/20, \pi/20]$.
5. If $\mathrm{RSS}_m[i] \geq \mathrm{RSS}_{m,\,\max}[i-1]$, then the Rx node updates $\mathrm{RSS}_{m,\,\max}[i] \geq \mathrm{RSS}_m[i], i_{\text{converge}} = 0$ and broadcasts a feedback bit of one to the Tx nodes, where $\mathrm{RSS}_m[i] = |y_m[i]|$ with $y_m[i] = |y_m[iT_s]|$.
6. Otherwise, the Rx node updates $i_{\text{converge}} = i_{\text{converge}} + 1$ and broadcasts a feedback bit of zero to the Tx nodes.
7. If the $n_k^{(m)}$-th Tx receives a feedback bit of one, then it updates $\theta_{n_k^{(m)},\,\max}[i] = \theta_{n_k^{(m)}}[i]$.
8. If $i_{\text{converge}} > I_{\text{threshold}}$ with a constant $I_{\text{threshold}}$, then terminate the algorithm.
9. Set $i = i + 1$ and return to Step 4.

One can see that Algorithm 2 is similar to Algorithm 1, but it is applied to a sub-cluster with a small number of Tx nodes, leading to fast convergence.

5.2 | Phase synchronization with one-bit feedback in inter-sub-clusters

In the inter-sub-cluster phase of synchronization, the following process is performed to adjust the sub-cluster phase $\left(a_k^{(m)}\right)$ of the k-th sub-cluster.

Algorithm 3. Inter-sub-cluster phase synchronization:

1. Initialize $a_k^{(m)}[0]=0$ and $a_{k,\max}^{(m)}[0]=0$ at the nodes in the k-th sub-cluster.
2. Create G grid points in [0, 2π] and set $\chi=2\pi/G$
3. Initialize at the data collector, where $\mathrm{RSS}_m[0]=\left|y_m[0]\right|=\left|s[0]\sum_{n=1}^{\bar{N}}d_{m,n}^{-\alpha}a_{m,n}e^{j(\phi_{m,n}+\theta_{n,\max})}+\nu_m[0]\right|$ and $\theta_{n,\max}$ is obtained via intra-sub-cluster phase synchronization. Set $i=1, i_{\text{convergence}}=0$, and $k=2$.
4. If the $n^{(m)}$-th node belongs to the k-th sub-cluster, it transmits a signal with a phase $\theta_{n^{(m)}}[i]=\theta_{n^{(m)},\max}+\alpha_k^{(m)}[i]$, where $\alpha_k^{(m)}[i]=\alpha_k^{(m)}[i-1]+\chi$ is obtained via intra-cluster phase synchronization.
5. If $\mathrm{RSS}_m[i]\geq\mathrm{RSS}_{m,\max}[i-1]$, the data collector updates $\mathrm{RSS}_{m,\max}[i]=\mathrm{RSS}_m[i]$ and $i_{\text{converge}}=0$, and broadcasts a feedback bit of one to the associated Rx nodes, where $\mathrm{RSS}_m[i]=\left|y_m[i]\right|$.
6. Otherwise, the data collector broadcasts a feedback bit of zero to the Rx nodes and updates $i_{\text{convergence}}=i_{\text{convergence}}+1$.
7. If the $n^{(m)}$-th node receives a feedback bit one, it updates $\alpha_{k,\max}^{(m)}[i]=\alpha_k^{(m)}[i]$.
8. Otherwise, the $n^{(m)}$-th node receives a feedback bit zero and it updates $\chi=-\chi$.
9. If $i_{\text{converge}}>I_{\text{threshold}}$ with a constant $I_{\text{threshold}}$, then set $k=k+1$.
10. Set $i=i+1$ and return to Step 4.

It should be noted that because the phases are already synchronized in each sub-cluster based on Algorithm 2, the inter-sub-cluster phase $a_k^{(m)}$ considers G grid points in [0, 2π], as shown in Algorithm 3. Figure 3 presents the variation in RSS according to α_2 in [0, 2π] for $K=2$. The changes in RSS exhibit the pattern of a sine wave. Accordingly, by using Algorithm 3, the peak RSS can be identified within several iterations.

To complete distributed beamforming, after performing clustering as discussed in Section 4, Algorithms 2 and 3 are repeated for each Rx node.

6 | ANALYSIS OF ENERGY HARVESTING OUTAGE PROBABILITIES

To analyze clustering performance, we analyze energy harvesting outage probabilities, which indicate that there are some Rx nodes that cannot satisfying the energy harvesting requirement P_{th}, which is defined as

$$\begin{aligned}P_{\text{out}}&\triangleq P\left(\left|y_{m,\text{converge}}\right|^2\leq P_{\text{th}},\exists m=1,\ldots,M\right)\\&=1-P\left(\min_{m=1,\ldots,M}\left|y_{m,\text{converge}}\right|^2>P_{\text{th}}\right)\\&=1-\prod_{m=1}^{M}P\left(\left|y_{m,\text{converge}}\right|^2>P_{\text{th}}\right),\end{aligned}\tag{10}$$

where $y_{m,\text{converge}}$ is the received signal at the m-th Rx node after Algorithms 2 and 3 and the clustering in described Section 4 are completed (ie, $\theta_{n_1^{(m)}}+\phi_{m,1}=\cdots=\theta_{n_{\tilde{n}}^{(m)}}+\phi_{m,1}$). Then, the received signal $y_{m,\text{converge}}$ can be written as

$$\left|y_{m,\text{converge}}\right|\approx\sqrt{P_{\text{tx}}}G_{m,\text{dbf}},\tag{11}$$

where $G_{m,\text{dbf}}=\sum_{l=1}^{\tilde{L}}d_{m,n_l^{(m)}}^{-\alpha/2}a_{m,n_l^{(m)}}$. It should be noted that $G_{m,\text{dbf}}$ can be regarded as a sum of weighted Rayleigh-distributed RVs. According to [17,18], $G_{m,\text{dbf}}$ can also be approximated as a Gamma-distributed RV. For example, in Figure 4, we generate

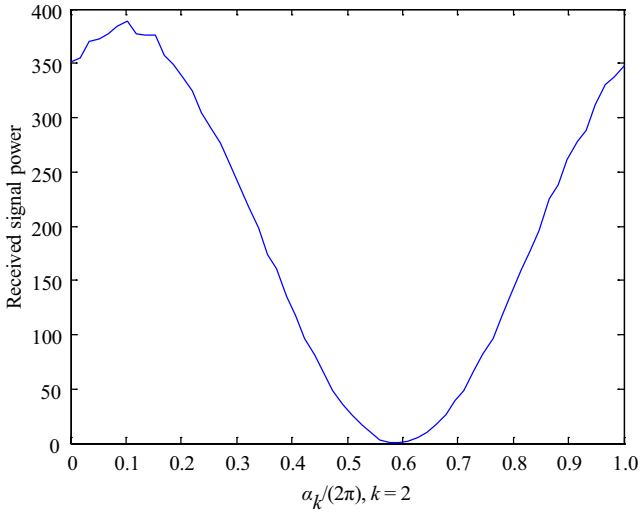

FIGURE 3 Variation in RSS according to α_2 in [0, 2π] for $K=2$

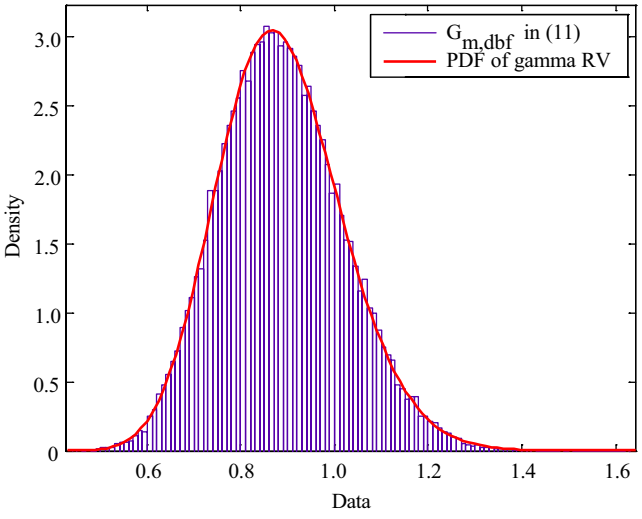

FIGURE 4 Histogram of random $G_{m,\text{dbf}}$ with $L=20$ and its approximation as the PDF of a gamma-distributed RV

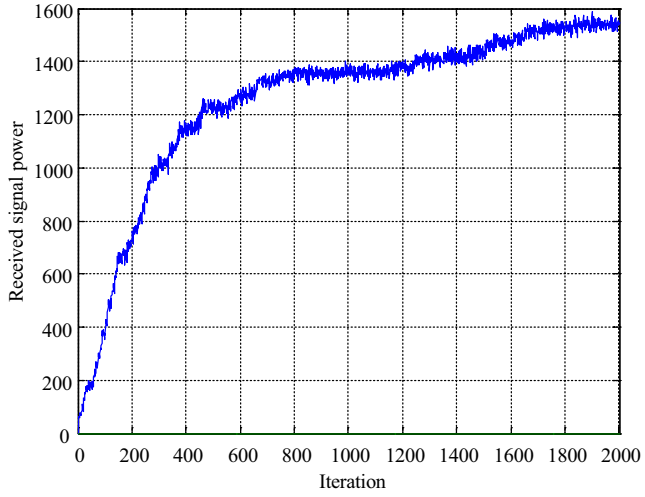

FIGURE 5 RSS when Algorithm 1 is exploited with $M = 1$ and $N = 40$

$h_{1,\,n_l}$ for $L = 20$ in (11) via Monte Carlo simulations and fit the resulting histogram with the probability density function (PDF) of a gamma-distributed RV as

$$f_{G_{m,\,\mathrm{dbf}}}(x) = \frac{1}{\Gamma(k_m)\theta_m^{k_m}} x^{k_m - 1} e^{\frac{x}{\theta_m}}, \tag{12}$$

where $\Gamma(z)$ is a Gamma function defined as $\Gamma(z) \triangleq \int_0^\infty x^{z-1}e^{-x}dx$. As shown in Figure 4, The histogram of the numerical results fits the analytic PDF of the Gamma RV. Here, the gamma PDF parameters k_m and θ_m, can be derived numerically from the long-term CSI $\left(d_{m,\,n_l^{(m)}}^{-\alpha/2}\right)$. Then, the outage probability in (10) can be defined as

$$\begin{aligned} P_{\mathrm{out}} &= 1 - \prod_{m=1}^{M} P\left(G_{m,\mathrm{dbf}} > \sqrt{\frac{P_{\mathrm{th}}}{P_{\mathrm{tx}}}}\right) \\ &= 1 - \prod_{m\,=\,1}^{M} \frac{1}{\Gamma(k_m)} \gamma\left(k_m,\ \frac{1}{\theta_m}\sqrt{\frac{P_{\mathrm{th}}}{P_{\mathrm{tx}}}}\right), \end{aligned} \tag{13}$$

where $\gamma(x, y)$ is an incomplete Gamma function defined as $\gamma(x, y) = \int_0^y t^{x-1}e^{-t}dt$. It should be noted that if an Rx node has information regarding large-scale fading $d_{1,\,n}^{-\alpha}$ for $n = 1, \ldots, N$, it can compute outage probabilities by approximating the distribution of harvested energy as a Gamma distribution, which can be exploited through the computation of the minimum required power for its serving Tx nodes.

7 | SIMULATION

In this section, we describe computer simulations conducted to verify the performance of the proposed algorithms.

To verify the effects of distributed beamforming with one-bit feedback alone, we consider a single Rx node and multiple Tx nodes. Because clustering is not required for a single Rx node, the convergence behavior of Algorithm 1 can be numerically analyzed in isolation.

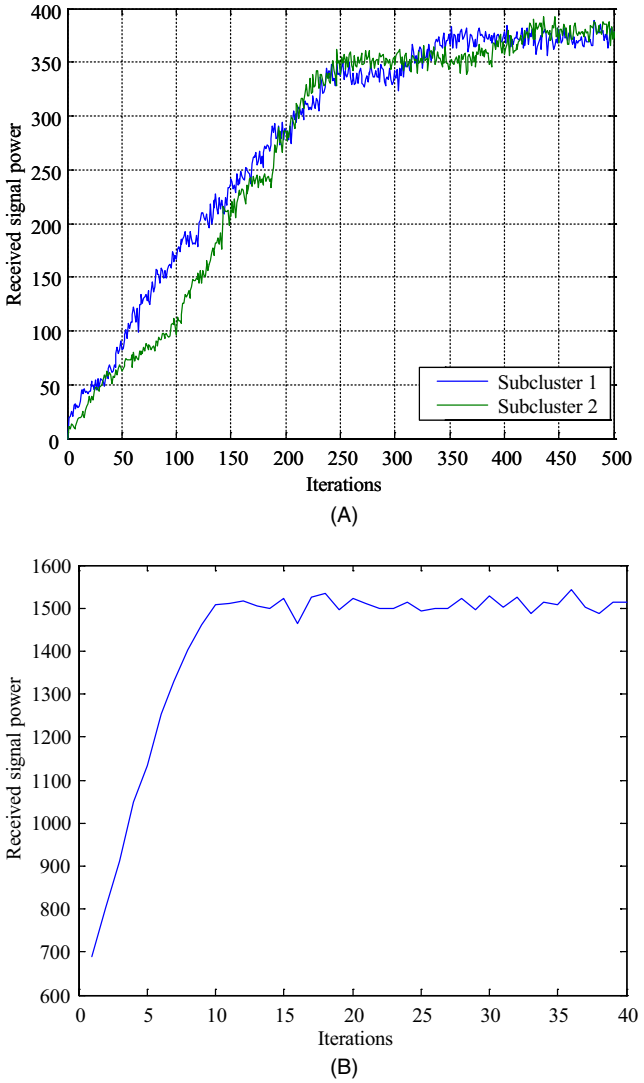

FIGURE 6 RSS when (A) the intra-sub-cluster phase is synchronized for each sub-cluster using Algorithm 2 and (B) the inter-sub-cluster phase is synchronized using Algorithm 3

All Tx nodes synchronize their transmitted signal phases according to single-bit feedback from a single Rx node, which implies that there is one cluster for distributed beamforming. Here, to determine whether Algorithm 1 can find the optimal phase for each energy Tx node in a distributed manner, we assume a unit amplitude of channel gain (ie, AWGN channel), unit distance for all Tx nodes (ie, $a_{1,\,n} = 1, d_{1,\,n} = 1$), and unit Tx power ($\mathrm{E}\left[\|s(t)\|^2\right] = 1$). Then, the optimal RSS can be denoted as N^2 for a single Rx node. Figure 5 presents the RSS values vs the number of iterations for Algorithm 1 with 40 Tx nodes (ie, $N = 40$). One can see that the RSS converges to the optimal value (ie, $N^2 = 1600$). Therefore, multiple Tx nodes can generate an effective energy beam to transfer energy to a

TABLE 1 Comparison of the required numbers of iterations for various numbers of Tx nodes

Number of Tx nodes (N)	Algorithm 1 # of iterations	Algorithms 2 and 3 with $K = 2$ # of iterations
$N = 20$	568	503
$N = 40$	1618	1070
$N = 60$	3496	1955
$N = 80$	6313	2930

given Rx node in a distributed manner using simple one-bit feedback that does not require any CSI at the Tx nodes.

Figure 6 presents the RSS vs the number of iterations for Algorithms 2 and 3 with 40 Tx nodes (ie, $N = 40$). Here, two sub-clusters are generated and each sub-cluster contains 20 Tx nodes. In Figure 6A, one can see that it requires approximately 400 iterations for the RSS to converge (ie, Tx nodes at each sub-cluster are synchronized). Additionally, Figure 6B presents the RSS when the inter-sub-cluster phases are synchronized using Algorithm 3. One can see that the RSS converges to the optimal value (ie, $N^2 = 1600$). According to Figures 5 and 6, the number of iterations required to achieve the optimal RSS value with Algorithm 1 is approximately 1800, whereas that with Algorithms 2 and 3 is $810 (= 400 \times 2(\text{Algorithm } 2) + 10(\text{Algorithm } 3))$. To evaluate performance precisely, in Table 1, we list the average numbers of required iterations for the RSS to converge for various numbers of Tx nodes. One can see that the proposed sub-clustering method (Algorithms 2 and 3) requires fewer iterations compared to Algorithm 1. As the number of Tx nodes increases, this gap becomes more apparent. Accordingly, by reducing the number of nodes that must be synchronized within a sub-cluster, we can accelerate the distributed beamforming process, which is desirable for massive IoT sensor networks.

To validate the effects of distributed beamforming using the clustering algorithms discussed in Section 4 in a general channel environment with multiple Rx nodes, we consider multiple Rx nodes and multiple Tx nodes with a Rayleigh fading channel. The path loss exponent is set to $\alpha = 3$. Figure 7 presents the RSS vs the number of iterations for the Rx node with the minimum RSS when the numbers of Tx nodes and Rx nodes are set to 36 and 3, respectively. Specifically, three Rx nodes are placed at $(x, y) = \{(5, 5), (5, 15), (15, 15)\}$ m and the Tx nodes are randomly placed in $[0, 14] \times [0, 14]$ m. Here, the distributed beamforming algorithm (Algorithm 1) is exploited with two different clustering methods: clustering based on path loss (Section 4.1) and weighted clustering based on path loss and the number of active serving Txs (Section 4.2). For the sake of comparison, we also evaluate the RSS for distributed beamforming without clustering. One can see that distributed beamforming with the proposed clustering methods yields a greater minimum RSS compared

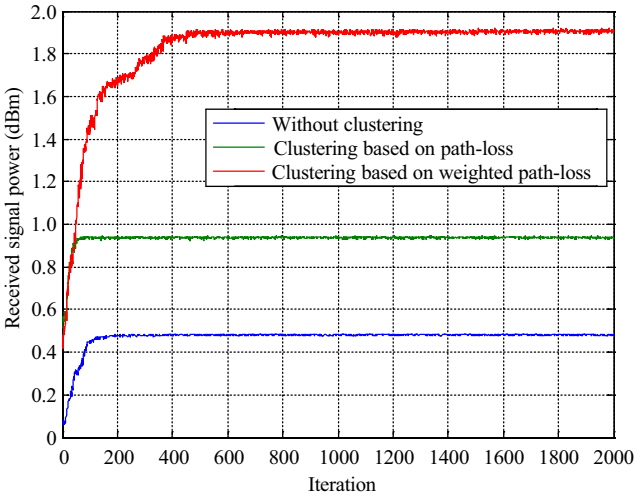

FIGURE 7 RSS at the Rx node with the minimum RSS when the numbers of Tx nodes and Rx nodes are 36 and 3, respectively

to conventional distributed beamforming without clustering. Additionally, the weighted clustering method described in Section 4.2 yields a greater minimum RSS compared to the clustering method based on path loss alone, indicating that energy outages can be reduced by using distributed beamforming with weighted clustering.

Figure 8 presents the RSS at all nodes vs the number of iterations when the numbers of Tx nodes and Rx nodes are 30 and 3, respectively, and the distributed beamforming

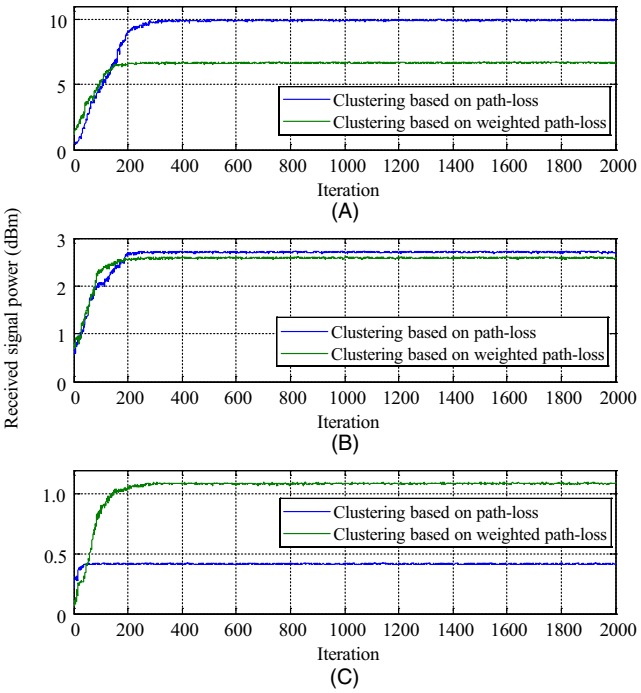

FIGURE 8 (A) RSS at the first Rx node, (B) second Rx node, and (C) third Rx node when the numbers of Tx nodes and Rx nodes are set to 30 and 3, respectively

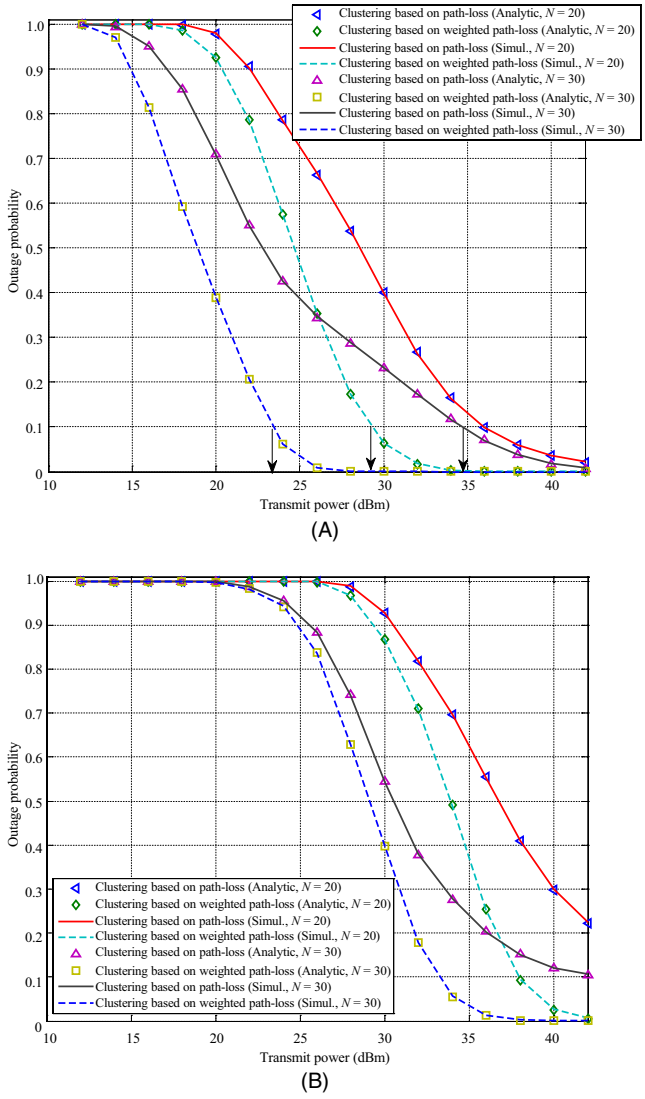

FIGURE 9 Energy outage probabilities when (A) $P_{th} = -10$ dBm and (B) $P_{th} = 0$ dBm with $M = 3$

algorithm (Algorithm 1) is exploited with the two proposed clustering methods. Here, the Tx power at each Tx node is set to 30 dBm. Because the numbers of Tx nodes associated with each Rx node and their path loss values for each Rx node differ, the RSS converges to different values at different Rx nodes. For the clustering based on path loss alone, the RSS at the third Rx node is <0.5 dBm because this node was selected by insufficient Tx nodes, resulting in an energy outage. In contrast, when weighted clustering based on path loss and the number of active serving Txs is exploited, the RSS at the third Rx node is >1.1 dBm. Therefore, we can conclude that weighted clustering based on path loss and the number of active serving Txs reduces energy outages in sensor networks, which coincides the observations in Figure 7.

In Figure 9, we evaluate the energy outage probabilities for distributed energy beamforming with the two different clustering methods discussed in Sections 4.1 and 4.2 when (a) $P_{th} = -10$ dBm and (b) $P_{th} = 0$ dBm with three Rx nodes and 20 or 30 energy Tx nodes. Here, the outage probabilities are numerically obtained using Monte Carlo simulations and the analytic results are plotted according to (13) in Section 6. In Figure 9A, as the Tx power or number of Tx nodes increases, the outage probability decreases. One can also see that when we exploit the weighted clustering method described in Section 4.2, we can drastically reduce the outage probability compared to the clustering method using only path loss. It should be noted that when $P_{th} = 0$ dBm (Figure 9B), the overall outage probability is greater than that when $P_{th} = -10$ dBm (Figure 9A).

In Figure 9, one can see that the simulation results coincide with the analytic results, indicating that analytic derivation can be exploited to determine the design parameters (eg, transmitted power, number of Rx nodes to be served) for wireless energy transfer networks with distributed beamforming. Specifically, we can determine the minimum Tx power when the minimum required power and outage probability constraints at Rx nodes are known. For example, when $P_{th} = -10$ dBm and $P_{out} = 0.1$ should be satisfied with $N = 30$, we should set the minimum Tx power at each Tx to 23 dBm with the weighted clustering method described in Section 4.2. In contrast, we should set the minimum Tx power to approximately 35 dBm with the clustering method described in Section 4.1. When $P_{th} = -10$ dBm and $P_{out} = 0.1$ should be satisfied with $N = 20$, we should set the minimum Tx power at each Tx to 28 dBm with weighted clustering. If we compare the sums of the required power levels for all Tx nodes, we require 28 dBm $\times$ 20 = 12.6 W for $N = 20$ and 23 dBm $\times$ 30 = 5.99 W for $N = 30$. Therefore, according to these analysis results, we can conclude that increasing node density is a more efficient method for deploying a wireless energy transfer network with distributed beamforming compared to increasing the transmitted power per Tx node. We can also determine how much Tx power is required to satisfy a given outage probability constraint, which is important for the design of wireless energy transfer networks with distributed beamforming.

8 | CONCLUSION

In this study, to overcome the energy depletion issue for sensor nodes, we developed a distributed beamforming method with one-bit feedback and clustering for multi-node wireless energy transfer. To transmit energy effectively, distributed Txs should adjust their transmitted signal phases properly such that their energy signals are constructively added at Rx nodes with the same phase, resulting in increased RSS. For multiple nodes, we proposed two clustering methods: clustering based solely on path loss and clustering based on both path loss and the numbers of active Txs serving Rx nodes.

We also proposed a fast distributed beamforming method based on Tx sub-clustering. Simulations demonstrated that our fast distributed energy beamforming with sub-clustering scheme has a short convergence time compared to a method without sub-clustering. This performance gap becomes more apparent for large numbers of cooperating nodes, meaning the proposed method is suitable for massive IoT sensor networks. By analyzing outage probabilities for distributed energy beamforming, we derived insights into the design of wireless energy transfer networks (ie, determination of the minimum required Tx power) and determined that increasing node density is a more efficient manner of deploying wireless energy transfer networks with distributed beamforming compared to increasing the transmitted power per Tx node.

ORCID

Jaehyun Park https://orcid.org/0000-0001-5327-9111

REFERENCES

1. I. F. Akyildiz et al., *A survey on sensor networks*, IEEE Commun. Mag. **40** (2002), 102–114.
2. A. J. Goldsmith and S. B. Wicker, *Design challenges for energy-constrained ad hoc wireless networks*, IEEE Wireless Commun. **9** (2002), 8–27.
3. S. Moon et al., *MAC protocol for energy efficiency and service differentiation with high goodput in wireless sensor networks*, IEICE trans. Commun. **E96-B** (2013), no. 6, 1444–1458.
4. J. Park and B. Clerckx, *Joint wireless information and energy transfer in a two-user MIMO interference channel*, IEEE Trans. Wireless Commun. **12** (2013), 4210–4221.
5. J. Park and B. Clerckx, *Joint wireless information and energy transfer in a k-user MIMO interference channel*, IEEE Trans. Wireless Commun. **13** (2014), 5781–5796.
6. J. Park and B. Clerckx, *Joint wireless information and energy transfer with reduced feedback in MIMO interference channels*, IEEE J. Select. Areas Commun. **33** (2015), 1563–1577.
7. S. H. Choi and D. I. Kim, *Multi-cell structure backscatter based wireless-powered communication network (WPCN)*, IEICE Trans. Commun. **E99-B** (2016), no. 8, 1687–1696.
8. J. Zhang et al., *Multi-antenna constant envelope wireless power transfer*, IEEE Trans. Green Commun. Netw. **1** (2017), 458–467.
9. B. Clerckx et al., *Fundamentals of wireless information and power transfer: From RF energy harvester models to signal and system designs*, IEEE J. Selected Areas Commun. **37** (2019), 4–33.
10. S. Bi, Y. J. A. Zhang, and R. Zhang, *Distributed scheduling in wireless powered communication network: Protocol design and performance analysis*, in Proc. Int. Symp. Modeling Optim. Mobilr, Ad Hoc, Wireless Netw. (Paris, France), May 2017, pp. 1–7.
11. S. Lee, J. Park, and J. Lee, *Joint information and energy packet scheduling in wireless powered sensor network*, IEICE Trans. Commun. **E101-B** (2018), no. 2, 520–527.
12. H. Lee and J. Lee, *Resource and task scheduling for SWIPT IoT system with renewable energy sources*, IEEE Internert Things J. **6** (2019), 2729–2748.
13. K. Snagaiah et al., *IoT resource allocation and optimization based on heuristic algorithm*, Sensors **20** (2020), no. 2, 539:1–26.
14. K. Sangaiah et al., *Energy consumption in point-coverage wireless sensor networks via Bat algorithm*, IEEE Access **7** (2019), 180258–180269.
15. R. Mudumbai et al., *Distributed beamforming using 1 bit feedback: From concept to realization*, in Proc. Allerton Conf. Commun., Contr., Comput. (Monticello, IL, USA), 2006.
16. J. Lee, S. Lee, and J. Park, *Fast phase synchronization with clustering and one-bit feedback for distributed beamforming in a wireless sensor network*, in Proc. IEEE Veh. Technol. Conf. (Porto, Portugal), June 2018, pp. 1–4.
17. M. F. Hanif, N. C. Beaulieu, and D. J. Young, *Two useful bounds related to weighted sums of Rayleigh random variables with applications to interference systems*, IEEE Trans. Commun. **60** (2012), 1788–1792.
18. G. Vegas-Snchez-Ferrero et al., *On the influence of interpolation on probabilistic models for ultrasonic images*, in Proc. IEEE Int. Symp. Biomed. Imag.: From Nano to Macro (Rotterdam, Netherlands), Apr. 2010, pp. 292–295.

AUTHOR BIOGRAPHIES

Jonghyeok Lee received his BS and MS degrees in electronic engineering from Pukyong National University in 2018 and 2020, respectively. His research interests include communication signal processing, wireless powered sensor networks, RADAR signal processing for automotive systems, and machine learning for radar and communication systems.

SeongJun Hwang received his BS degree in electronic engineering from Pukyong National University in 2020. His research interests include communication signal processing, OFDM radar, and machine learning for communication systems.

Yong-gi Hong received his BS degree in electronic engineering from Pukyong National University in 2020. His research interests include signal processing for wireless communications, interference cancelation and resource allocation, and machine learning for communication systems.

Jaehyun Park received his BS degree and PhD (MS-PhD joint program) in electrical engineering from the Korea Advanced Institute of Science and Technology in 2003 and 2010, respectively. From 2010 to 2013, he was a senior researcher at the Electronics

and Telecommunications Research Institute, where he worked on transceiver design and spectrum sensing for cognitive radio systems. From 2013 to 2014, he was a postdoctoral research associate at the Electrical and Electronic Engineering Department of the Imperial College of London. He is currently an associate professor at the Electronic Engineering Department of Pukyong National University, South Korea. His research interests include signal processing for wireless communications and radar systems with a focus on detection and estimation for MIMO systems, MIMO radar, cognitive radio networks, and joint information and energy transfer.

Woo-Jin Byun received his BS degree in electronic engineering from the Kyungpook National University, Daegu, Korea, in 1992, and his MS degree and PhD in electrical engineering from the Korea Advanced Institute of Science and Technology, Daejeon, Korea, in 1995 and 2000, respectively. In 1999, he joined the Samsung Electro-Mechanics Company, Suwon, Korea, where he developed mobile communication devices, such as power amplifiers and radio modules, from 1999 to 2004. He worked with the Athena group at the Georgia Institute of Technology as a visiting scholar from 2015 to 2016. He is currently serving as Assistant Vice President for the Radio Satellite Research Division at ETRI. His current research interests include RF/millimeter-wave/THz integrated circuits and systems (communication and RADAR) designs, planar and reflector antennas, and electromagnetic scattering analysis.